European Journal of Pharmacology 757 (2015) 59–67

Contents lists available at ScienceDirect

European Journal of Pharmacology

journal homepage: www.elsevier.com/locate/ejphar

Molecular and cellular pharmacology

SIRT1 inhibition in pancreatic cancer models: Contrasting effects *in vitro* and *in vivo*

Chern Ein Oon [a,b,*], Carina Strell [a], Keng Yoon Yeong [b], Arne Östman [a], Jai Prakash [a,c,*]

[a] Department of Oncology & Pathology, Cancer Center Karolinska, Karolinska Institutet, 171 76 Stockholm, Sweden
[b] Institute for Research in Molecular Medicine, Universiti Sains Malaysia, 11800 Minden, Penang, Malaysia
[c] Targeted Therapeutics, Department of Biomaterials Science and Technology, MIRA Institute for Biomedical Technology and Technical Medicine, University of Twente, Zuidhorst building, ZH254, 7500AE Enschede, The Netherlands

ARTICLE INFO

Article history:
Received 4 August 2014
Received in revised form
25 March 2015
Accepted 25 March 2015
Available online 3 April 2015

Chemical compounds studied in this article:
6-Chloro-2,3,4,9-tetrahydro-1H-Carbazole-1-carboxamide (EX527) (PubChem CID: 5113032)

Keywords:
Pancreatic cancer
EX527
SIRT1
Sirtuin
Gemcitabine
Tumour resistance

ABSTRACT

Gemcitabine remains the standard treatment for pancreatic cancer, although most patients acquire resistance to the therapy. Up-regulated in pancreatic cancer, SIRT1 is involved in tumorigenesis and drug resistance. However the mechanism through which SIRT1 regulates drug sensitivity in cancer cells is mainly unknown. We hypothesise that inhibiting SIRT1 activity may increase sensitivity of pancreatic cancer cells to gemcitabine treatment through the regulation of apototic cell death, cell cycle, epithelial-mesenschymal-transition (EMT) and senescence. We demonstrate that gemcitabine or 6-Chloro-2,3,4,9-tetrahydro-1 H-Carbazole-1-carboxamide (EX527) SIRT1 inhibitor reduces PANC-1 cell proliferation *in vitro*. EX527 enhanced sensitivity of PANC-1 cells to gemcitabine treatment through increased apoptosis. However, EX527 displayed no beneficial effect either as a monotreatment or in combination with gemcitabine in the modulation of cell cycle progression. Combination treatment did not reverse the two phenomena known to affect drug sensitivity, namely EMT and senescence, which are both induced by gemcitabine. Unexpectedly, EX527 promoted PANC-1 xenograft tumour growth in SCID mice compared to control group. Dual tX527 and gemcitabine displayed no synergistic effect compared to gemcitabine alone. The study reveals that SIRT1 is involved in chemoresistance and that inhibiting SIRT1 activity with EX527 sensitised PANC-1 cells to gemcitabine treatment *in vitro*. Sensitisation of cells is shown to be mainly through induction of micronuclei formation as a result of DNA damage and apoptosis *in vitro*. However, the absence of positive combinatorial effects *in vivo* indicates possible effects on cells of the tumor microenvironment and suggests caution regarding the clinical relevance of tissue culture findings with EX527.

1. Introduction

Pancreatic cancer is one of the most aggressive malignancies. Gemcitabine is an analogue of deoxycytidine and a pyrimidine antimetabolite which remains the cornerstone for pancreatic cancer patients as first-line therapy. Nevertheless, many patients develop resistance to existing therapeutic regimes, hence understanding the mechanisms involved in mediating chemoresistance in pancreatic cancer could pave way for novel therapies. The tumour spectrum of epigenetic and genetic alterations may be accountable for poor patient prognosis and survival rate. Sirtuin 1 (SIRT1) is the mammalian ortholog of the yeast silent information regulator 2 (SIR2) which has been described as being upregulated in many cancer types including pancreatic cancer (Ashraf et al., 2006; Huffman et al., 2007; Zhao et al., 2011).

Modulation of SIRT1 has been proposed in cancer therapy (Ota et al., 2006) although its biological function is further complicated by its paradox as either a tumor suppressor or tumor promoter depending on cancer types (Roth and Chen, 2013). SIRT1 over-expression has been demonstrated to reduce intestinal (Firestein et al., 2008) and liver (Herranz et al., 2010) tumour formation in mice models, suggesting that SIRT1 may suppress tumour formation. Nevertheless, SIRT1 has been implicated in tumorigenesis and drug resistance through deacetylation of p53 (Vaziri et al., 2001), PTEN (Ikenoue et al., 2008), nuclear factor-kappaB (Yeung

* Corresponding author at: Institute for Research in Molecular Medicine, Universiti Sains Malaysia, 11800 Penang, Malaysia. Tel.: +604 6534879.
* Corresponding author at: Targeted Therapeutics, Department of Biomaterials, Science and Technology, MIRA Institute for Biomedical Technology and Technical Medicine, University of Twente, Zuidhorst building, ZH254, 7500AE Enschede, The Netherlands. Tel.: +31534893096.
E-mail addresses: chern.oon@usm.my (C.E. Oon), j.prakash@utwente.nl (J. Prakash).

http://dx.doi.org/10.1016/j.ejphar.2015.03.064
0014-2999/

et al., 2004), Bax/Bcl-2 (Qiao et al., 2006) and E2F1 transcription factor (Wang et al., 2006). A growing body of evidence has linked the acquisition of epithelial-mesenchymal transition (EMT) of cancer cells (Chen et al., 2011; Meng and Wu, 2012; Rosano et al., 2011) and drug induced senescence (Achuthan et al., 2011; Zhang et al., 2014) to chemoresistance. EMT is a phenomenon that enables tumour epithelial cells to take on a mesenchymal cell phenotype, resulting in increased tumour cell migration, promotion of invasiveness and enhanced resistance to cell death (Vega et al., 2004). SIRT1 has been reported to favour EMT through cooperation with EMT transcription factors to repress E-cadherin expression in epithelial cells (Nieto, 2013). Cellular senescence confers to tumour resistance, likely through induction of cell cycle arrest which decreases the sensitivity of tumour cells to chemotherapeutic drugs which are designed to target fast dividing cancer cells (Gordon and Nelson, 2012). The connection between SIRT1 and cellular senescence is one that has been well established by various studies (Ota et al., 2006; Zhang et al., 2014; Zu et al., 2010).

Suppression of SIRT1 expression at the transcript level led to apoptosis, cell cycle arrest and senescence with reported further enhancement of pancreatic cancer cell sensitivity to gemcitabine treatment *in vitro* (Zhao et al.). However, this study was limited to *in vitro* experiments and *in vivo* effects thus remain unknown. Therefore, in this study we aim to investigate the combinational effect of this inhibitor on the efficacy of gemcitabine in pancreatic cancer cell line *in vitro and in vivo* by employing a well-known SIRT1 inhibitor, Chloro-2,3,4,9-tetrahydro-1 H-Carbazole-1-carboxamide (EX527) which has been used in clinical trials for Huntington's disease (see the Siena Biotech website[1]).

2. Material and methods

2.1. Cell culture

PANC-1 pancreatic cancer cells were obtained from American Type Culture Collection (ATCC) and maintained in Roswell Park Memorial Institute (RPMI) 1640 medium (GIBCO) supplemented with 10% Foetal Calf Serum (GIBCO), 100 units/ml penicillin (GIBCO) and 100 units/ml streptomycin (GIBCO). Cells were kept at 37 °C in a humidified 5% CO_2 atmosphere.

2.2. Cell treatment

PANC-1 cells were plated at appropriate density in RPMI media supplemented with 10% FCS according to assays. After 24 h, the cells were treated with DMSO (Sigma) as vehicle control, 6-Chloro-2,3,4,9-tetrahydro-1 H-Carbazole-1-carboxamide (EX527) (Sigma) and gemcitabine (Selleckchem) in RPMI media containing 1% FCS. Media and treatment were renewed every 3 days.

2.3. SIRT1 activity

SIRT1 activity was tested using the Fluor de Lys kit (Biomol International) according to standard manufacturer's protocol. Fluorescence was measured at 360 nm (excitation) and 460 nm (emission) on a fluorometric reader (Infinite 200 TECAN) and the inhibition was expressed in arbitrary unit for that of SIRT1 activity under each experimental condition. Resveratrol (Sigma) was used as a positive control in addition to Nicotinamide (provided in the kit) as negative control.

[1] http://www.sienabiotech.it/index.jsp

2.4. Caspase 3/7 activity assay

Cells were subjected to Caspase 3/7 activities measurement with Caspase-Glo assay kit (Promega) according to standard manufacturer's protocol. Briefly, plates were equilibrated to room temperature 30 min before measurement. The cells were rinsed once with PBS. A volume of 50 μl of media in addition to 50 μl of Caspase-Glo 3/7 reagent was added to each well. The plate was then incubated at room temperature for 2 h. The luminescence was measured in a plate-reader (Thermo Labsystems) using parameters of 1 min lag time and 1 s/well read time.

2.5. Cell viability assay

The extent of proliferation was determined by comparing cell counts for samples treated with EX527 and/or gemcitabine (as mentioned above) with untreated controls at different time points (Day 3, 6 and 9) using CyQUANT® assay (Life Technologies). PANC-1 cells were plated at 2.5×10^3 cells per well in a 96-well microplate. Cells were incubated with CyQUANT reagent according to the standard manufacturer's protocol. Fluorescence intensities of samples were measured with a fluorescence microplate reader (Infinite 200 TECAN) using excitation at 485 nm and fluorescence detection at 530 nm.

2.6. Western blot

PANC-1 cells were cultured at 2×10^5 cells/dish in 6-well plates in RPMI media overnight and treated as above. Protein lysates were obtained from harvested cells at different time points (Day 3, 6 and 9). Briefly, protein extractions from cultured cells were performed using urea lysis buffer which consists of 10% glycerol, 10 mM Tris–HCl (pH 6.8), 5 mM dithiothreitol, 1% sodium dodecyl sulphate (SDS) and 8 M urea. Protein was quantified using a NanoDrop ND-1000 spectrophotometer using absorbance at 280 nm (Thermo Scientific). The cell lysates were resolved by SDS-PAGE on NuPAGE® Bis–Tris Pre-Cast Gels (Life Techonologies). Proteins were then transferred from the gel to an Immobilon-polyvinylidene fluoride transfer membrane (Millipore, Watford). Non-specific binding sites on the membrane were blocked for 1 h at room temperature in blocking solution (5% milk powder, 0.1% Tween-20 in PBS). After blocking, the membrane was probed with a primary antibodies (Cleaved PARP, SIRT1 and Vimentin; Cell Signalling Technology, beta actin; Sigma) in blocking solution overnight at 4 °C. The membrane was then rinsed in PBS with 0.1% Tween-20 three times for 10 min each. Next, the membrane was probed with an appropriate HRP-conjugated secondary antibody in blocking solution for 1 h at room temperature. The blots were detected using Amersham ECL western blotting detection reagents (GE Healthcare) and visualised using a CCD camera.

Densitometry analysis was performed using Image J by calculating the relative density of each peak which corresponds well with the size and intensity of each band in the western blot, and normalised to the standard (first lane) and the loading control (β-Actin). Analyses were carried out on data from three independent experiments.

2.7. Quantitative real-time PCR

RNA was harvested from PANC-1 cells 24 h post-treatment using TRI Reagent according to the manufacturer's protocol. Reverse transcription was carried out using the High Capacity cDNA Reverse Transcription Kit (Applied Biosystems, Warrington). Real-time PCR quantitative (QPCR) was performed using Applied Biosystem 7500 Fast Real-time PCR System. The cDNA samples were then put through 40 cycles of amplification at 95 °C for 15 s

followed by 60 °C for 1 min. The mRNA level of SIRT1 was determined through normalisation to Glyceraldehyde 3-phosphate dehydrogenase (GAPDH) using the following primers:

SIRT1: Forward: 5′- TGGCAAAGGAGCAGATTAGTAGG-3′
Reverse: 5′- CTGCCACAAGAACTAGAGGATAAGA-3′
GAPDH: Forward: 5′- TGAACGGGAAGCTCACTGG-3′
Reverse: 5′- TCCACCACCCTGTTGCTGTA-3′)

Analyses were carried out on data from three independent experiments.

2.8. Senescence assay

Briefly, PANC-1 cells were seeded in 6-well plates at 2×10^4 cells per well and treated accordingly as mentioned above. Senescence—associated beta gal (SA-β galactosidase) activity was detected by incubating fixed cells with the chromogenic β gal substrate X-gal in a buffer at pH 6.0 overnight at 37 °C, according to the manufacturer's protocol (Cell Signalling Technology). After 24 h, the cells were washed with phosphate-buffered saline (PBS) and viewed under the inverted bright field microscope. The proportion of cells positive for SA-βgal activity was expressed as the ratio of blue cells (senescent cells) over the total number of cells. Analyses were carried out on data from three independent experiments.

2.9. Immunocytofluorescence

Cells were seeded onto glass slips in 6-well plates at 2×10^4 cells per well and treated as above. The cells were rinsed briefly in PBS and fixed with 4% formaldehyde in PBS for 15 min at room temperature followed by rinsing three times in PBS for 5 min each. Cells were permeabilised with ice-cold 100% methanol and incubated for 10 min at −20 °C before final rinse in PBS for 5 min. Following blocking of nonspecific binding with 5% BSA in PBS for 1 h, sections were incubated with primary antibody for 1 h at room temperature. The cells were then incubated at 4 °C overnight followed by secondary antibody for a1 h at room temperature. Slides were mounted using fluorescent mounting medium with diamidinophenolindole DAPI (Vectashield) to stain the DNA. The numbers of cells with micronuclei were expressed as percentage of micronucleated cells over total number of cells. The AxioVision Rel. 4.6 Software (Carl Zeiss) was used for visualisation. Analyses were carried out on data from three independent experiments.

2.10. Immunohistochemistry

Frozen sections were fixed with acetone for 10 min and left to air dry for 1 h at room temperature. Sections were blocked for unspecific binding with 5% bovine serum albumin (SIGMA) for 1 h followed by incubation with SIRT1 rabbit monoclonal antibody (1:500, Cell Signalling Technology #2496S). Slides were rinsed in PBS for 5 min followed by Anti rabbit polymer IMMPRESS Reagent (Vector Labs) for 30 min, and then rinsed in PBS for 5 min. Visualisation of SIRT1 was achieved by applying diaminobenzidine substrate (DAB) for 8 min and further rinsed in PBS. Sections were counter stained with hematoxylin and mounted in Aquamount and visualised under a light microscope. The AxioVision Rel. 4.6 Software (Carl Zeiss) was used for visualisation. Analyses were carried out on seven xenograft sections per group. Semi-quantitative scoring was done by ranking the SIRT1 expression according to abundance and intensity.

2.11. Cell cycle assay

1×10^5 PANC-1 were seeded in 1% FCS containing RPMI media and treated with 4 nM gemcitabine and 1 μM EX527 alone or in combination. Treatment was renewed every third Day. Cell membranes were lysed with a hypotonic buffer (4 mM Sodium Citrate, 0,1% Triton X-100) containing 0,1 mM propidium iodide (PI) and 50 μg/ml RNaseA (Life Technologies) for 20 min at 4 °C under mild agitation. Aggregates were removed by filtration trough a 40 μm cell strainer. The total nuclei fluorescence FL2-A was measured under exclusion of debris/aggregates *via* the FL2-W *versus* FL2-A plot using the FACS Calibur (BD Biosciences). The data was analysed with the ModFIT Cell Cycle analysis software (Verity Software House). One way ANOVA was performed to analyse group differences.

2.12. Animal experiments

Six- to seven-week-old male BALB/c SCID mice (Harlan Sprague Dawley, Inc., Indiana) were injected subcutaneously with 1:1 ratio of cell suspension containing 5×10^6 PANC-1 cells and Matrigel (BD Biosciences). Each treatment group consisted of seven mice. Tumour growth was monitored two to three times per week by measuring the length (L), width (W) and height (H) of each tumour with a calliper. Tumour volumes (V) were then calculated from the formula ($V = 0.52 \times L \times W \times H$). Treatments with PBS (control), gemcitabine (50 mg/kg or 25 mg/kg), EX527 (10 mg/kg) or in combination were given intraperitoneally every three days, starting from Day 7, when the tumours reached the size of 50 mm^3 until the mice were sacrificed. Mice were euthanized when three tumours from any group attained 1000 mm^3 tumour volume.

2.13. Statistical methods

The statistical analysis and graphing software Excel (Microsoft, USA) and Prism (GraphPad, USA) were used to analyse all data. The Student's *t*-test was used to compare mean values between two data sets. The analysis of variance (ANOVA) test was used to compare mean values among three or more data sets, and the Bonferroni's post-test was used to compare any two data sets among the three or more sets. Kruskal–Wallis test with Dunn's post-test comparison was employed to analyse more than two sets of non-parametric data. The ANOVA *F*-test was used to assess significance between two curve fits. Statistical significance was indicated in the figures by *, where $P < 0.05$, and**, where $P < 0.01$. All error bars depict S.E.M.

2.14. Animal ethic statement

The animal experiments were executed in strict accordance with the National guidelines and approved by the Stockholm North Ethical Committee on Animal Experiments and the Karolinska animal ethics review boards (NR166/12). All steps were taken to curtail mice suffering.

3. Results

3.1. Gemcitabine increased SIRT1 expression in PANC-1 cells.

PANC-1 pancreatic cancer cells were treated with GEM (4 nM). Both gene and protein expression analyses showed increased SIRT1 expression in PANC-1 cell lines after the treatment with GEM (Fig. 1). The immunofluorescent staining showed the induced nuclear expression of SIRT1 in PANC-1 after activation with GEM. These data indicate that GEM induces SIRT1 expression and potentially SIRT1-mediated pathways.

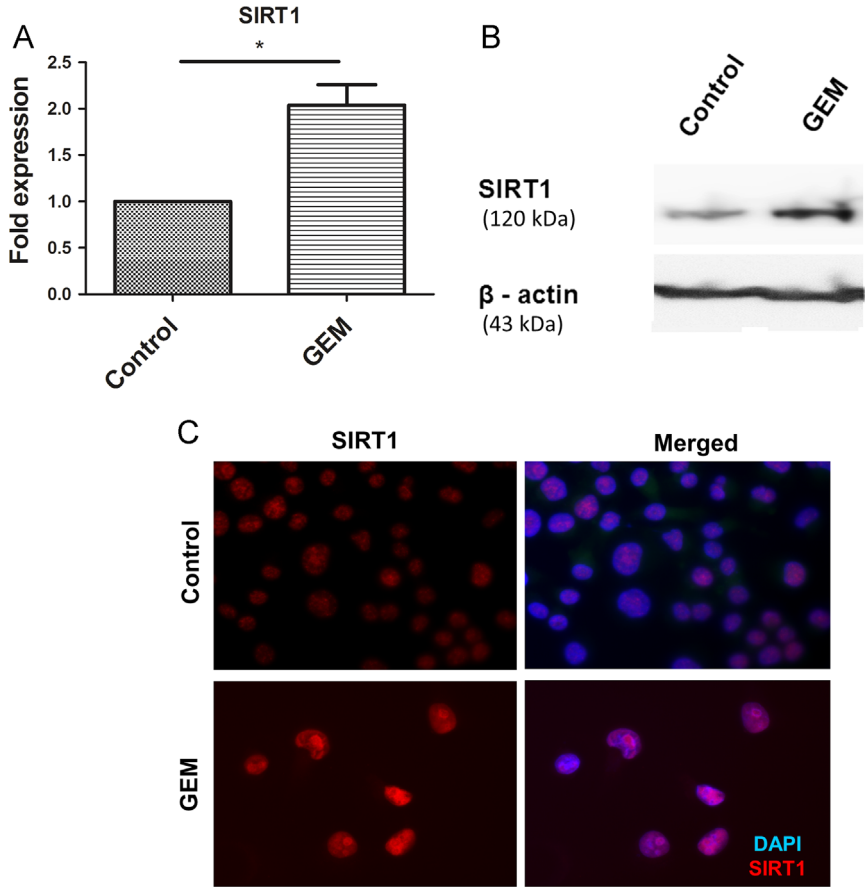

Fig. 1. Up-regulation of SIRT1 expression in PANC-1 cells upon treatment with gemcitabine (GEM). PANC- cells were treated with GEM (4 nM) for 48 h or 72 h and subjected to gene (48 h) and protein (72 h) expression analysis by quantitative RT-PCR (A), western blot (B) and immunofluorescent staining (400 × magnification) (C), β-actin was used as loading control. A representative figure for immunofluorescence and western blot is shown. Graph is shown as average from three independent experiments. Data are presented as mean ± S.E.M. (*, $P < 0.05$; Student t test).

3.2. *Inhibition of SIRT1 using EX527 increased PANC-1 cell sensitivity to gemcitabine*

We confirmed EX527 as an inhibitor of SIRT1 activity using the *in vitro* Fluor de Lys deacetylation assay (Fig. S1). The cell proliferation of PANC-1 cells was evaluated using CyQuant Cell Proliferation Assay kit. To explore synergistic effects of EX527 and GEM, optimal dosage for EX527 and gemcitabine (GEM) was established *via* dose response analyses (EX527: 0, 0.2, 1.0 and 10.0 μM; GEM: 0, 4, 20 and 50 nM) on Day 3 (Fig. S3). The proliferation of cells was significantly inhibited in a dose dependent manner with GEM but not with EX527. We found 1 μM EX527 in combination with 4 nM GEM to be most optimal in reducing cell viability on Day 3 (Fig. S3), in which their effects were synergistic as determined by the combination index of less than 1 using the Calcusyn 2.1 software (Table S1). We proceeded with a time course experiment over 9 days to test viability of the cells using EX527 (1 μM) and the minimal effective dose for GEM (4 nM) (Fig. 2A). PANC-1 cells displayed significantly reduced cell viability when treated with EX527 or GEM compared to Control, with EX527 enhancing chemosensitivity of the cells towards GEM on Day 9 (Fig. 2B).

3.3. *EX527 induced apoptosis and micronuclei formation in GEM-treated PANC-1 cells*

To investigate the mechanism of action involved in EX527-induced sensitisation of PANC-1 to GEM, we carried out assays to determine their effects on apoptosis, micronuclei formation, cell cycle distribution, senescence and EMT. As shown in Fig. 2, GEM but not EX527 increased percentage of Caspase 3/7 activity (Fig. 2C) and the protein expression of cleaved PARP (Fig. 2D) compared to control cells on Day 9. Furthermore, synergistic activation of Caspase 3/7 and increase in cleaved PARP expression by EX527 and GEM combination treatment was also detected on Day 9 (Fig. 2C and D).

The micronucleus assay is often used as a tool for genotoxicity assessment of various compounds. To assess the extent of chromosomal damage caused by GEM and EX527, we assayed PANC-1 cells for micronuclei formation after exposure to treatments for a period of 6 and 9 days, during which upon cell division DNA damage resulted in formation of smaller micronuclei apart from the main nucleus. Micronucleus assay results were most prominent on Day 6 (Fig. 3A). GEM treatment alone promoted micronuclei formation compared to Control (Fig. 3A). This was further enhanced by treatment combined with EX527. During the course of treatment, GEM and combination treatment induced nuclear blebbing in PANC-1 cells (Fig. 3), which visually corroborate promotion of apoptotic activity in the cells.

To explore the effect of EX527 and/or GEM on PANC-1 cell cycle, cells were assayed for cell cycle distribution after 3 (figure not shown), 6 (figure not shown) and 9 days post-treatment (Fig. S6). At EX527 (1 μM) and GEM (4 nM), their effects on cell cycle modulation were not additive at these time points, suggesting that cell cycle arrest is not an apparent contributing factor to reduced cell viability observed with combination treatment.

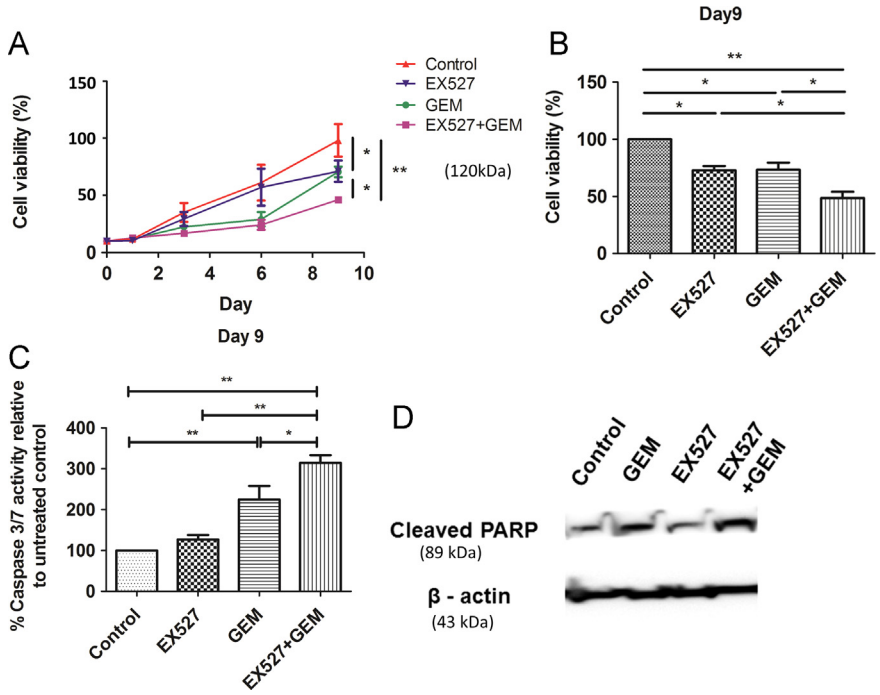

Fig. 2. Enhancement of PANC-1 cell sensitivity to GEM (4 nM) by EX527 (1 μM). Cell proliferation and viability was determined using CyQuant cell proliferation assay (A). Both EX527 and GEM reduce cell viability compared to control and synergistically reduce cell viability compared to single treatment of either one at Day 9 (B) through induction of apoptosis as depicted by Caspase 3/7 assay (C) and western blot for Cleaved PARP (D) at Day 9. β-actin was used as loading control. A representative figure for western blot is shown. Graphs are shown as average from three independent experiments. Data are presented as mean ± S.E.M. (*, $P < 0.05$, **, $P < 0.01$; ANOVA).

3.4. *Effect of gemcitabine and EX527 on cellular senescence and epithelial-mesenchymal-transition (EMT)*

Cellular senescence was determined using SA-β-gal staining on Day 6 (Fig. 4A) and Day 9 (Fig. 4B). EX527 and GEM alone induced cellular senenscence compared to Control, however their combination treatment did not result in any synergistic effect (Fig. 4). The effect of EX527 and GEM on EMT in PANC-1 cells was assessed on Day 3. At lower concentration, GEM (4 nM) did not induce EMT (data not shown). EX527 (1 μM) had no effect on EMT whereas GEM (50 nM) induced EMT in PANC-1 cells as characterised by reduced cyokeratin expression (Fig. 5A), change of cell morphology (spindle shape) (Fig. 5B) and increased vimentin expression (Fig. 5C). Combination treatment had no synergistic effect compared to single treatment of either one.

3.5. *In vivo monotherapy with EX527 promoted tumour growth in vivo*

PANC-1 cells were grown as subcutaneous xenograft tumours in mice to investigate the translational benefit of combination treatment for EX527 and GEM. We performed two sets of experiments using different dosages of GEM. Surprisingly, EX527 (10 mg/kg, i.p.) promoted tumour growth *in vivo* which is in contrast of the *in vitro* findings. GEM at two different doses 50 mg/kg and 25 mg/kg (Figs. 6A and B, respectively) effectively hampered tumour growth (Fig. 6). Combination treatment of GEM and EX527 did not result in any synergistic effect in tumour growth but followed the trend of GEM alone-induced effect (Fig. 6). Immunohistochemical staining revealed unaltered SIRT1 expression in EX527 group compared to Control (Fig. S5), confirming the *in vitro* analysis of SIRT1 expression in PANC-1 cells treated with EX527 (Fig. S4). GEM treatment was found to induce SIRT1 expression in the xenograft tumours compared to Control group; the SIRT1 expression remains high in combination group (Fig. S5).

4. Discussion

Combination therapies are by far the most promising strategy in pancreatic cancer. SIRT1 expression is elevated in pancreatic cancer tissues (Zhao et al., 2011). Its expression is found to be further enhanced by GEM (Fig. 1 and Fig. S5), as also observed by others (Zhang et al., 2014). As SIRT1 is known to interact with targets that are directly involved in cell growth, genome integrity, cell cycle progression, senescence and cell death (Kabra et al., 2009; Wang et al., 2006), we focused on these avenues to dissect the mechanisms of SIRT1 mediating chemosensitivity to GEM. We demonstrated the beneficial effect of inhibiting SIRT1 activity using EX527 in combination to GEM, resulting in reduced cell viability *in vitro* (Fig. 2A and B), confirming other findings (Zhang et al., 2014).

At lower effective doses, we found the beneficial effect of EX527 on sensitisation of PANC-1 cells to GEM to be mediated through apoptosis, as depicted by increase in Caspase3/7 activity (Fig. 2C) and cleaved PARP expression (Fig. 2D). Interestingly, EX527 as a single agent did not induce apoptosis in contrast to findings from other SIRT1 inhibition studies (Gong et al., 2013; Zhang et al., 2014). The downstream events of SIRT1 regulation may be dependent on fine-tuned expression or activity of SIRT1, hence the lower effective dose used in our experiment may not be strong enough to elicit cell death through apoptosis. Characteristics of apoptosis comprise of nuclear envelope degradation and nuclear blebbing, resulting in the formation of micronuclei (Fig. 3). A micronucleus is an erratic nucleus that is formed during the anaphase of mitosis, resulting in development of chromosome fragments with nuclear membranes in daughter cells, apart from the main nucleus. SIRT1 has been shown to protect against DNA damage through multiple targets, including the p53 molecule (Chen et al., 2005), hence inhibition of SIRT1 is expected to result in increased DNA damage. SIRT1 inhibitor alongside other HDAC inhibitors have been shown to induce DNA damage in different cell types (Gorenne et al., 2012; Robert et al., 2011). However, in our experiments EX527 (1 μM) was not found to stimulate the formation of micronuclei

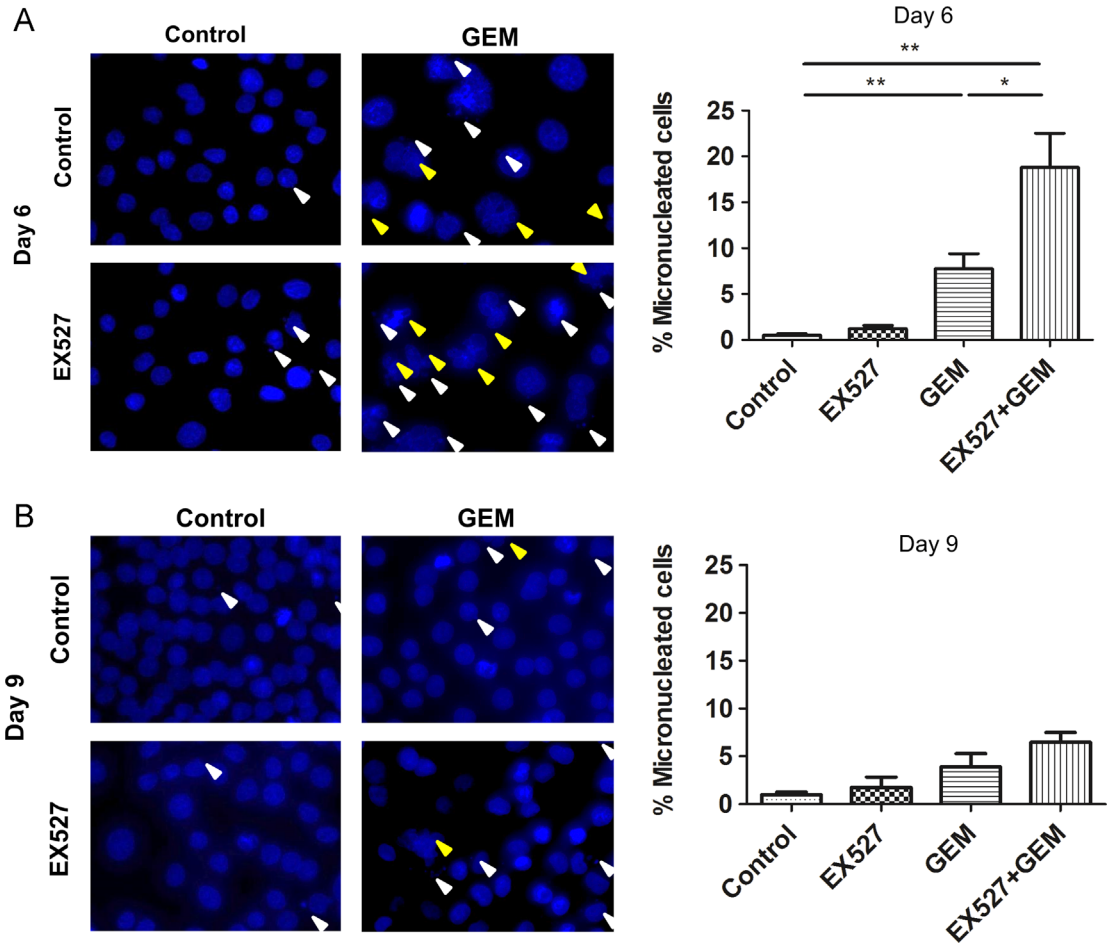

Fig. 3. Induction of DNA damage by EX527 (1 μM) and GEM (4 nM) as depicted by micronuclei formation (white arrowhead) and nuclear blebbing in PANC-1 cells (yellow arrowhead) characterising apoptosis at Day 6 (A) and Day 9 (B) (400× magnification) (C). A representative figure for immunofluorescence from three independent experiments is shown. Data are presented as mean ± S.E.M. (*, $P < 0.05$, **, $P < 0.01$; ANOVA). (For interpretation of the references to colour in this figure legend, the reader is referred to the web version of this article.)

as a result of DNA damage on Day 6 and Day 9 (Fig. 3), possibly due to low used concentrations. DNA- damaging agents including GEM have been established to induce micronuclei formation (Aydemir and Bilaloglu, 2003; Yu et al., 2013). This is corroborated by our observation in PANC-1 cells on Day 6 despite using low concentration of GEM (4 nM) as also reported by Yu and colleagues using ovarian cancer cells (Yu et al., 2013) (Fig. 3A). Further increase in frequency of micronuclei was demonstrated in the EX527 and GEM combination treatment group on Day 6 (Fig. 3A), again suggesting that SIRT1 may mediate chemoresistance in PANC-1 and inhibition of SIRT1 sensitises cells to GEM. A decrease in micronuclei formation on Day 9 might be due to the induction of apoptosis in many of the cells that had shown micronuclei formation on Day 6.

SIRT1 regulation of cell proliferation is expected to act alongside a modulation of cell cycle, mainly through the deacetylation and inhibition of E2F1 and retinoblastoma protein (pRb) (Kabra et al., 2009). EX-527 treatment of serum-starved HCT116 cells resulted in hyper-phosphorylation of Ser-795 on pRb (Kabra et al., 2009; Wang et al., 2006). However, the optimal combination effect of EX527 (1 μM) and GEM (4 nM) (Table S1) on cell cycle modulation in PANC-1 cells were rather minimal (Fig. S6), suggesting that cell cycle arrest is not a contributing factor to reduced cell viability (Fig. 2A), although higher doses of treatment were found to cause cell cycle arrest in the same cell line (Zhang et al., 2014). When a higher concentration of GEM (50 nM) was employed, we obtained a strong S-Phase arrest 24 h post-treatment (Fig. S6B), as also demonstrated by others in PANC-1 cells using higher concentrations of GEM (Giovannetti et al., 2004; Morgan et al., 2005). The differences in the effect of EX527 (Zhang et al., 2014) and GEM (Giovannetti et al., 2004; Morgan et al., 2005) on cell cycle arrest could be attributed to the differences in working concentrations and time point when the assays were carried out.

Drug-induced senescence has been reported to confer to tumour resistance, providing an escape for cancer cells to evade cell death (Achuthan et al., 2011). Cellular senescence is defined as an irreversible withdrawal from cell cycle, rendering the cancer cells to remain static in growth. Inhibition of SIRT1 using different modulators and silencing SIRT1 at the gene level have been shown to promote cellular senescence in human cancer cells (Ota et al., 2006; Zhang et al., 2014; Zhao et al., 2011). Our results indicated enhanced senescence by GEM and EX527 alone compared to Control on Day 6 (Fig. 4A) and Day 9 (Fig. 4B), through increased senescence-associated β-galactosidase [SA-β-GAL] activity. However, no combination effect was observed in dual treatment group (Fig. 4), which is in contrast to a recent study with reported further enhancement of cellular senescence in a combination group which utilised higher doses of EX527 and GEM (Zhang et al., 2014). Altogether, these suggest that level of SIRT1 inhibition may be crucial in deciding the mechanisms involved in cell survival.

Although emerging evidence has linked SIRT1 to EMT in different cell types, either as a positive driver or a negative regulator (Byles et al., 2012; Simic et al., 2013), this was surprisingly not observed in our experiments. Lower concentration of GEM did not stimulate EMT (data not shown) in PANC-1 cells,

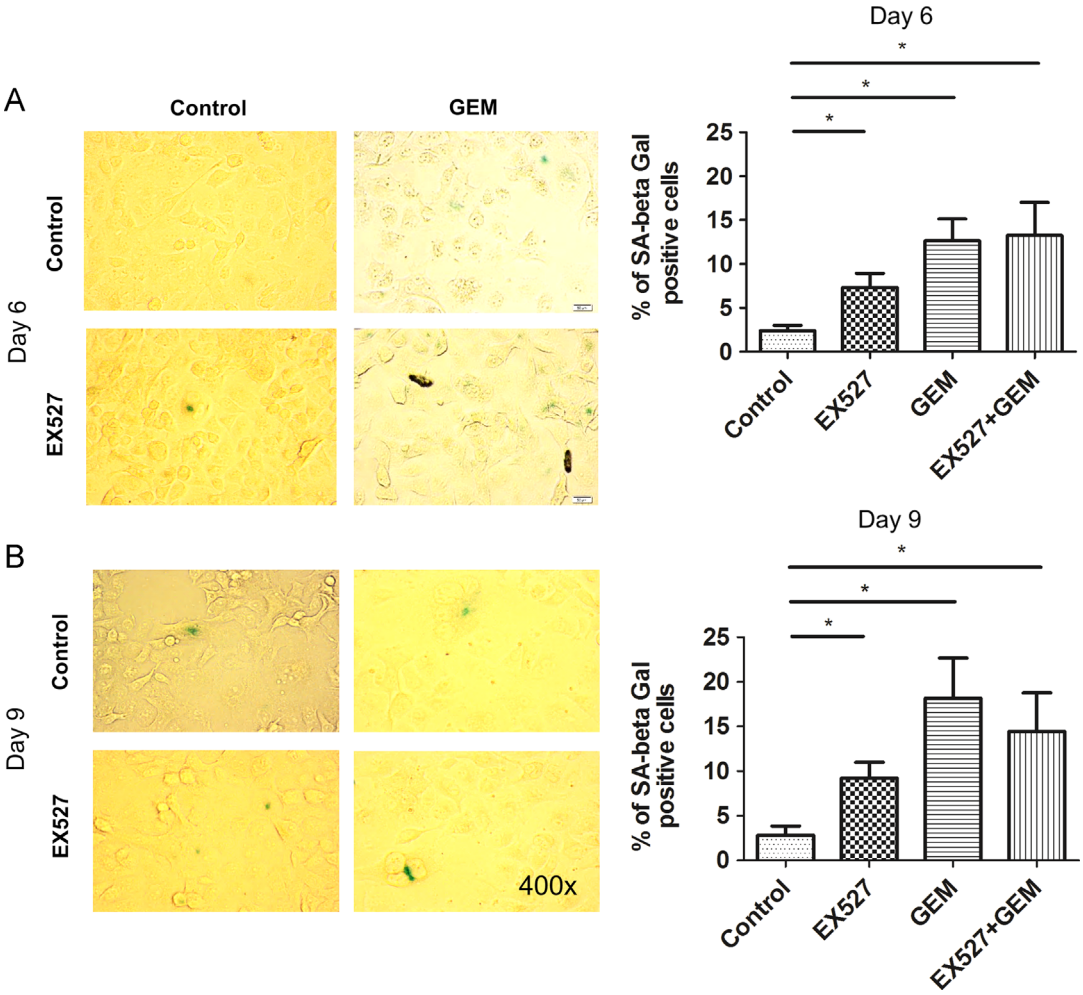

Fig. 4. Stimulation of drug-induced senescence by GEM in PANC-1 with no observed additional effect on cellular senescence in EX527 (1 μM) and GEM (4 nM) combination treatment. Senescence-associated-β-gal activity was measured at Day 6 (A) and Day 9 (B) and scored as percentage of SA- β-gal positive cells (blue) over total cells. A representative figure for senescence-associated-β-gal staining is shown (400 × magnification). Graphs are shown as average from three independent experiments. Data are presented as mean ± S.E.M. (*, $P < 0.05$; ANOVA). (For interpretation of the references to colour in this figure legend, the reader is referred to the web version of this article.)

hence we investigated the effect of EX527 in combination with a higher dose of GEM (50 nM) (Fig. 5). There was no effect on EMT with EX527 treatment alone (Fig. 5). Induction of EMT by GEM remained unperturbed by EX527 (Fig. 5), implying that EMT is the unlikely explanation for SIRT1 mediated chemosensitivity to GEM in PANC-1 cells.

Despite having tumour cell growth inhibition and enhanced combination effects with GEM *in vitro*, the inhibition of SIRT1 in a pancreatic tumour model *in vivo* turned to be controversial. We tested the effect of EX527 alone and in combination with GEM in pancreatic xenograft tumour model. Surprisingly, EX527 alone was found to enhance the tumour growth instead of inhibiting the tumour growth as expected considering the *in vitro* data (Fig. 6). Moreover, no therapeutic benefit was observed in combination treatment group. These data is in contrary to the results reported by Gong et al. (2013) in which they reported tumour growth inhibition using Sirtinol, another SIRT1 inhibitor, together with gemcitabine in a syngeneic pancreatic tumour model . Many reasons could account for this. One of such is that Sirtinol is an inhibitor of both SIRT1 and SIRT2 in contrast of EX527 that is highly specific against SIRT1 (Fig. S2). This may account for the different results observed (Gong et al., 2013), highlighting the importance of combined inhibitory effects of SIRT1 and SIRT2 activities through fine-tuned selectivity. In addition to the unchanged level of SIRT1 expression in EX527 group compared to Control group, the high SIRT1 expression in combination treatment group (Fig. S2) indicates that EX527 had no effect on SIRT1 expression but exerted its effect through modulating SIRT1 activity. It is likely that effective inhibitory effect of SIRT1 may also depend on the molecular mechanism which encompasses of complex compensatory mechanism between different Sirtuin proteins as well as the distribution of other Sirtuins and the downstream targets. Furthermore, the SIRT1 inhibition in other cell types in the tumor microenvironment such as immune cells, endothelial cells and tumour-associated fibroblasts might be responsible for the observed tumor-promoting effect. However, the latter statement needs further investigations.

5. Conclusion

SIRT1 inhibitors such as Sirtinol and Cambinol have been reported to have therapeutic effects on tumour cells through induction of growth arrest, senescence, or cell death in tumour cells (Heltweg et al., 2006; Ota et al., 2006). The detailed mechanistic basis for these effects is difficult to define due to limited specificity of these compounds which, at the conditions used, may have different effects on different Sirtuins. In addition, the discrepancy between our *in vitro* and *in vivo* results is also compatible with additional effects of Sirtuin-inhibitors on the tumor microenvironment which will affect the ultimate therapeutic outcome. Further studies are thus needed to understand

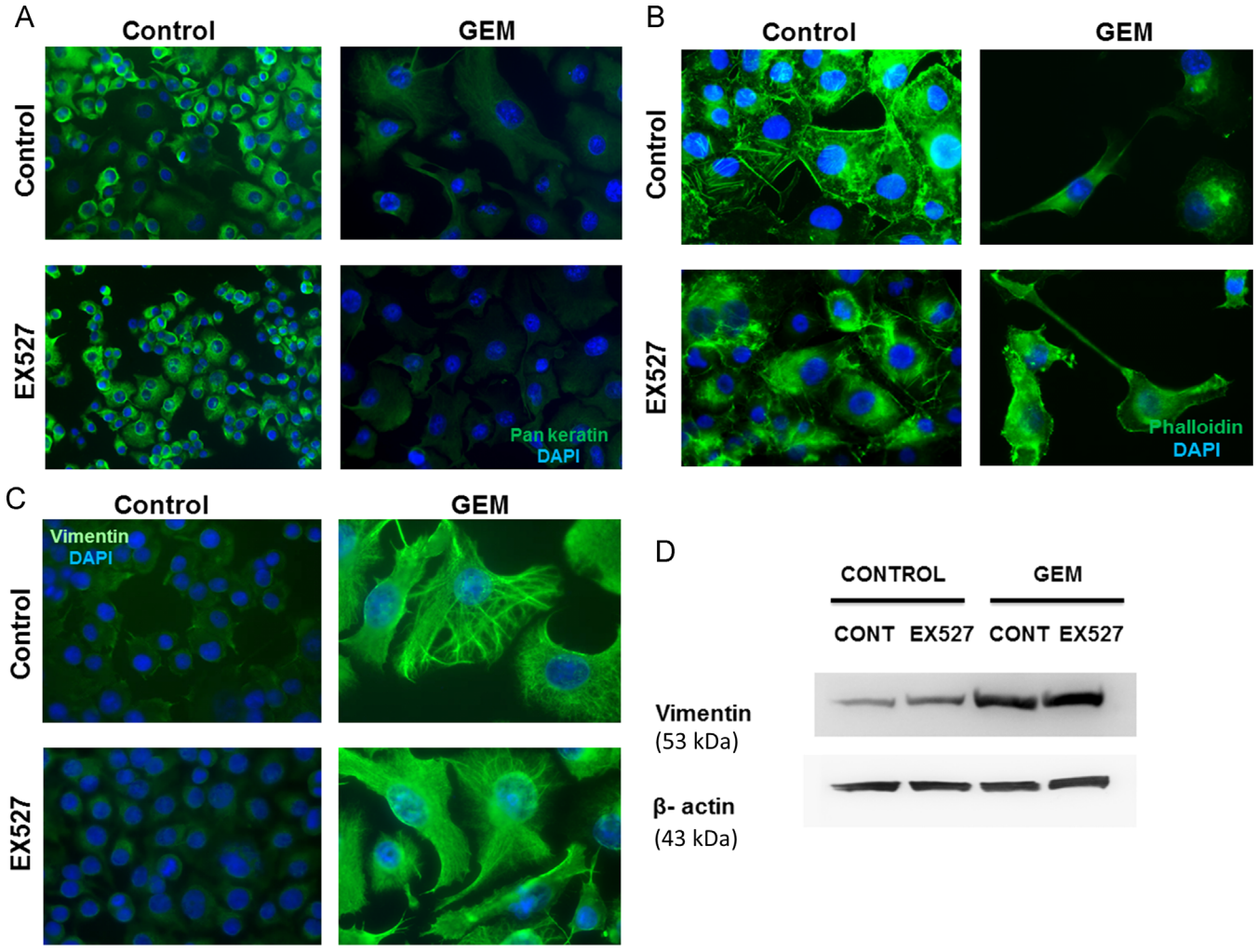

Fig. 5. Effect of EX527 (1 μM) and GEM (50 nM) on epithelial-mesenchymal-transition (EMT). Immunofluorescent staining and western blot were carried out after 72 h treatment. Features of EMT include loss of epithelial cytokeratin expression (200 × magnification) (A), prominent elongated spindle-shaped cells as depicted by phalloidin staining (200 × magnification) (B) and increase in vimentin expression (400 × magnification) (C). Western blot analyses showing the vimentin expression and β-actin was used as a loading control (D). A representative figure from three independent experiments is shown.

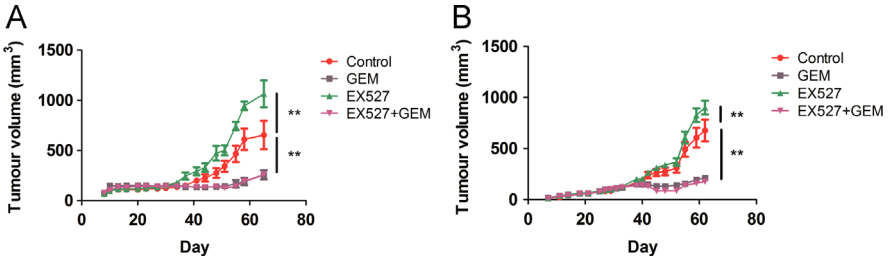

Fig. 6. PANC-1 xenograft tumour growth curves using EX527 (10 mg/kg) and different GEM dosage regimens; 50 mg/kg (A) and 25 mg/kg (B). EX527 promoted PANC-1 tumour growth in both sets of experiments. No synergistic effect was observed in EX527/GEM combination treatment. Data are presented as mean ± S.E.M. (**, $P < 0.01$; *F*-test).

the mechanisms driven by the janus-faced SIRT1 and its oncogenic crosstalk with other pathways.

Disclosure of potential conflicts of interest

No potential conflicts of interest were disclosed.

Financial disclosure

C.E.O was supported by Universiti Sains Malaysia Short Term Grant (304/CIPPM/6312135) and Fundamental Research Grant Scheme (FRGS) Malaysia (203/CIPPM/6711335). J.P was funded by Swedish Research Council young researcher project grant (621-2011-5389). The funders played no role in study design, data analysis or preparation of the manuscript.

Acknowledgements

The authors thank Anna-Karin Persson and Kenth Andersson for excellent technical assistance with animal work. We also extend our gratitude to Professor Lars-Gunnar Larsson for useful advice on senescence. C.E.O was supported by USM, Malaysia short

term Grant 304/CIPPM/6312135 and FRGS Grant 203/CIPPM/6711335. J.P. was funded by Swedish Research Council young researcher project grant (621-2011-5389). K.Y.Y was supported by the Ministry of Education (Malaysia), Malaysia MYBRAIN15 scholarship.

Appendix A. Supporting information

Supplementary data associated with this article can be found in the online version at http://dx.doi.org/10.1016/j.ejphar.2015.03.064.

References

Achuthan, S., Santhoshkumar, T.R., Prabhakar, J., Nair, S.A., Pillai, M.R., 2011. Drug-induced senescence generates chemoresistant stemlike cells with low reactive oxygen species. J. Biol. Chem. 286, 37813–37829.

Ashraf, N., Zino, S., Macintyre, A., Kingsmore, D., Payne, A.P., George, W.D., Shiels, P.G., 2006. Altered sirtuin expression is associated with node-positive breast cancer. Br. J. Cancer 95, 1056–1061.

Aydemir, N., Bilaloglu, R., 2003. Genotoxicity of two anticancer drugs, gemcitabine and topotecan, in mouse bone marrow *in vivo*. Mutat. Res. 537, 43–51.

Byles, V., Zhu, L., Lovaas, J.D., Chmilewski, L.K., Wang, J., Faller, D.V., Dai, Y., 2012. SIRT1 induces EMT by cooperating with EMT transcription factors and enhances prostate cancer cell migration and metastasis. Oncogene 31, 4619–4629.

Chen, W.Y., Wang, D.H., Yen, R.C., Luo, J., Gu, W., Baylin, S.B., 2005. Tumor suppressor HIC1 directly regulates SIRT1 to modulate p53-dependent DNA-damage responses. Cell 123, 437–448.

Chen, X., Lingala, S., Khoobyari, S., Nolta, J., Zern, M.A., Wu, J., 2011. Epithelial mesenchymal transition and hedgehog signalling activation are associated with chemoresistance and invasion of hepatoma subpopulations. J. Hepatol. 55, 838–845.

Firestein, R., Blander, G., Michan, S., Oberdoerffer, P., Ogino, S., Campbell, J., Bhimavarapu, A., Luikenhuis, S., de Cabo, R., Fuchs, C., Hahn, W.C., Guarente, L.P., Sinclair, D.A., 2008. The SIRT1 deacetylase suppresses intestinal tumorigenesis and colon cancer growth. PLoS One 3, e2020.

Giovannetti, E., Mey, V., Danesi, R., Mosca, I., Del Tacca, M., 2004. Synergistic cytotoxicity and pharmacogenetics of gemcitabine and pemetrexed combination in pancreatic cancer cell lines. Clin. Cancer Res. 10, 2936–2943.

Gong, D.J., Zhang, J.M., Yu, M., Zhuang, B., Guo, Q.Q., 2013. Inhibition of SIRT1 combined with gemcitabine therapy for pancreatic carcinoma. Clin. Interv. Aging 8, 889–897.

Gordon, R.R., Nelson, P.S., 2012. Cellular senescence and cancer chemotherapy resistance. Drug Resist. Updates 15, 123–131.

Gorenne, I., Kumar, S., Gray, K., Figg, N., Yu, H., Mercer, J., Bennett, M., 2012. Vascular smooth muscle cell sirtuin 1 protects against DNA damage and inhibits atherosclerosis. Circulation 127, 386–396.

Heltweg, B., Gatbonton, T., Schuler, A.D., Posakony, J., Li, H., Goehle, S., Kollipara, R., Depinho, R.A., Gu, Y., Simon, J.A., Bedalov, A., 2006. Antitumor activity of a small-molecule inhibitor of human silent information regulator 2 enzymes. Cancer Res. 66, 4368–4377.

Herranz, D., Munoz-Martin, M., Canamero, M., Mulero, F., Martinez-Pastor, B., Fernandez-Capetillo, O., Serrano, M., 2010. Sirt1 improves healthy ageing and protects from metabolic syndrome-associated cancer. Nat. Commun. 1, 3.

Huffman, D.M., Grizzle, W.E., Bamman, M.M., Kim, J.S., Eltoum, I.A., Elgavish, A., Nagy, T.R., 2007. SIRT1 is significantly elevated in mouse and human prostate cancer. Cancer Res. 67, 6612–6618.

Ikenoue, T., Inoki, K., Zhao, B., Guan, K.L., 2008. PTEN acetylation modulates its interaction with PDZ domain. Cancer Res. 68, 6908–6912.

Kabra, N., Li, Z., Chen, L., Li, B., Zhang, X., Wang, C., Yeatman, T., Coppola, D., Chen, J., 2009. SirT1 is an inhibitor of proliferation and tumor formation in colon cancer. J. Biol. Chem. 284, 18210–18217.

Meng, F., Wu, G., 2012. The rejuvenated scenario of epithelial-mesenchymal transition (EMT) and cancer metastasis. Cancer Metastasis Rev. 31, 455–467.

Morgan, M.A., Parsels, L.A., Parsels, J.D., Mesiwala, A.K., Maybaum, J., Lawrence, T.S., 2005. Role of checkpoint kinase 1 in preventing premature mitosis in response to gemcitabine. Cancer Res. 65, 6835–6842.

Nieto, M.A., 2013. Epithelial plasticity: a common theme in embryonic and cancer cells. Science 342, 1234850.

Ota, H., Tokunaga, E., Chang, K., Hikasa, M., Iijima, K., Eto, M., Kozaki, K., Akishita, M., Ouchi, Y., Kaneki, M., 2006. Sirt1 inhibitor, Sirtinol, induces senescence-like growth arrest with attenuated Ras-MAPK signalling in human cancer cells. Oncogene 25, 176–185.

Qiao, A.M., Ikejima, T., Tashiro, S., Onodera, S., Zhang, W.G., Wu, Y.L., 2006. Involvement of mitochondria and caspase pathways in N-demethyl-clarithromycin-induced apoptosis in human cervical cancer HeLa cell. Acta Pharmacol. Sin. 27, 1622–1629.

Robert, T., Vanoli, F., Chiolo, I., Shubassi, G., Bernstein, K.A., Rothstein, R., Botrugno, O.A., Parazzoli, D., Oldani, A., Minucci, S., Foiani, M., 2011. HDACs link the DNA damage response, processing of double-strand breaks and autophagy. Nature 471, 74–79.

Rosano, L., Cianfrocca, R., Spinella, F., Di Castro, V., Nicotra, M.R., Lucidi, A., Ferrandina, G., Natali, P.G., Bagnato, A., 2011. Acquisition of chemoresistance and EMT phenotype is linked with activation of the endothelin A receptor pathway in ovarian carcinoma cells. Clin. Cancer Res. 17, 2350–2360.

Roth, M., Chen, W.Y., 2013. Sorting out functions of sirtuins in cancer. Oncogene 33, 1609–1620.

Simic, P., Williams, E.O., Bell, E.L., Gong, J.J., Bonkowski, M., Guarente, L., 2013. SIRT1 suppresses the epithelial-to-mesenchymal transition in cancer metastasis and organ fibrosis. Cell Rep. 3, 1175–1186.

Vaziri, H., Dessain, S.K., Ng Eaton, E., Imai, S.I., Frye, R.A., Pandita, T.K., Guarente, L., Weinberg, R.A., 2001. hSIR2(SIRT1) functions as an NAD-dependent p53 deacetylase. Cell 107, 149–159.

Vega, S., Morales, A.V., Ocana, O.H., Valdes, F., Fabregat, I., Nieto, M.A., 2004. Snail blocks the cell cycle and confers resistance to cell death. Genes Dev. 18, 1131–1143.

Wang, C., Chen, L., Hou, X., Li, Z., Kabra, N., Ma, Y., Nemoto, S., Finkel, T., Gu, W., Cress, W. D., Chen, J., 2006. Interactions between E2F1 and SirT1 regulate apoptotic response to DNA damage. Nat. Cell Biol. 8, 1025–1031.

Yeung, F., Hoberg, J.E., Ramsey, C.S., Keller, M.D., Jones, D.R., Frye, R.A., Mayo, M.W., 2004. Modulation of NF-kappaB-dependent transcription and cell survival by the SIRT1 deacetylase. EMBO J. 23, 2369–2380.

Yu, L., Zhao, Y., Quan, C., Ji, W., Zhu, J., Huang, Y., Guan, R., Sun, D., Jin, Y., Meng, X., Zhang, C., Yu, Y., Bai, J., Sun, W., Fu, S., 2013. Gemcitabine eliminates double minute chromosomes from human ovarian cancer cells. PLoS One 8, e71988.

Zhang, J.G., Hong, D.F., Zhang, C.W., Sun, X.D., Wang, Z.F., Shi, Y., Liu, J.W., Shen, G.L., Zhang, Y.B., Cheng, J., Wang, C.Y., Zhao, G., 2014. Sirtuin 1 facilitates chemoresistance of pancreatic cancer cells by regulating adaptive response to chemotherapy-induced stress. Cancer Sci. 105, 445–454.

Zhao, G., Cui, J., Zhang, J.G., Qin, Q., Chen, Q., Yin, T., Deng, S.C., Liu, Y., Liu, L., Wang, B., Tian, K., Wang, G.B., Wang, C.Y., 2011. SIRT1 RNAi knockdown induces apoptosis and senescence, inhibits invasion and enhances chemosensitivity in pancreatic cancer cells. Gene Ther. 18, 920–928.

Zu, Y., Liu, L., Lee, M.Y., Xu, C., Liang, Y., Man, R.Y., Vanhoutte, P.M., Wang, Y., 2010. SIRT1 promotes proliferation and prevents senescence through targeting LKB1 in primary porcine aortic endothelial cells. Circ. Res. 106, 1384–1393.